

Wide-dynamic-range sensors

Orly Yadid-Pecht, MEMBER SPIE
Ben-Gurion University of the Negev
Electrical and Computer Engineering
Department
P.O. Box 653
Beer-Sheva 84105
Israel
E-mail: oyp@ee.bgu.ac.il

Abstract. The work done to provide image sensors (CCDs and CMOS) with a wide dynamic range is reviewed. The different classes of solutions, which consist of logarithmic sensors, "clipped" sensors, multimode sensors, frequency-based sensors, and sensors with control over integration time are described. The pros and cons of each solution are discussed, and some new experimental results are shown. Active pixel sensors with a wide dynamic range are analyzed and possible future directions are pointed out. © 1999 Society of Photo-Optical Instrumentation Engineers. [S0091-3286(99)01610-4]

Subject terms: image sensors; wide dynamic range; detector arrays; image quality; image reconstruction; very large scale integration; complementary metal oxide semiconductor image sensor; charge-coupled device; active pixel sensor.

Paper 980463 received Dec. 14, 1998; revised manuscript received Apr. 19, 1999; accepted for publication Apr. 29, 1999.

1 Introduction

Scenes imaged with electronic cameras can have a wide range of illumination depending on lighting conditions. Scene illuminations range from 10^{-3} lx for night vision, 10^2 to 10^3 lx for indoor lighting, to 10^5 lx for bright sunlight, to higher levels for direct viewing of other light sources such as oncoming headlights. The intrascene dynamic range capability of a sensor is measured as $20 \log(S/N)$, where S is the saturation level and N is the root mean square (rms) read noise floor measured in electrons or volts. Typical charge-coupled devices (CCDs) and CMOS active pixel sensors (APSs) have a dynamic range of 65 to 75 dB. For dynamic range improvement, two methods are considered. One is to reduce noise and expand the dynamic range toward darker scenes. The other is to expand incident light saturation level, and improve the dynamic range toward brighter scenes. We concentrate here on the latter. Brighter scenes, or wide variations in intrascene illumination, can arise in several situations. One example has already been mentioned, night driving. Another commonly occurring situation is when taking a picture of a person standing in front of a window. Other situations include the observation of a landing aircraft, metrology, or astronomy. Since this limitation is very apparent, various solutions have been proposed to cope with it, in both CCD and CMOS technologies.

Previously suggested solutions for widening the dynamic range can be divided into

1. companding sensors, such as logarithmic, compressed response photodetectors
2. "clipped" sensors, as in CCDs with antiblooming structures, where the response curve is clipped
3. multimode sensors, that have been shown in CMOS where operation modes were changed
4. frequency-based sensors, where the sensor output is converted to pulse frequency
5. external control over integration time, which can be

further divided to

- global control, where the whole sensor can have different integration time
 - local control, where different areas within the sensor can have different exposure times
6. autonomous control over integration time, in which the sensor itself provides the means of different integration times.

This paper reviews the existing solutions for the limited dynamic range in CCD and CMOS technologies, with emphasis on the recent solutions in APS technology. Experimental results of the latter are shown and advantages and limitations are discussed as well as future possible directions.

2 Companding Sensors

Compressing the response curve is usually done through a sensor with a logarithmic response. This approach has advantages such as increased dynamic range, reduced susceptibility to blooming, and fewer ADC bits for digital output. The logarithmic sensors work in continuous, i.e., nonintegrating mode, and therefore can have a higher time sampling resolution per pixel if required.

Chamberlain and Lee¹ were the first to suggest this kind of reading, via a phototransistor they called PHOTOFET (see Fig. 1 left side; the subsequent stages described in Fig. 1 explain the antiblooming feature this device also has. The antiblooming is explained later). The PHOTOFET consists of a photodiode and a diode-connected metal-oxide semiconductor (MOS) transistor. The output voltage (V) of the photodiode is logarithmically dependent on the light intensity, due to the subthreshold operation of the diode connected MOS transistor. The output voltage is given by

$$V = V_1 \ln(I_s / I_{ph}),$$

where V_1 is the dark voltage, I_s is the leakage current, and I_{ph} is the photocurrent.

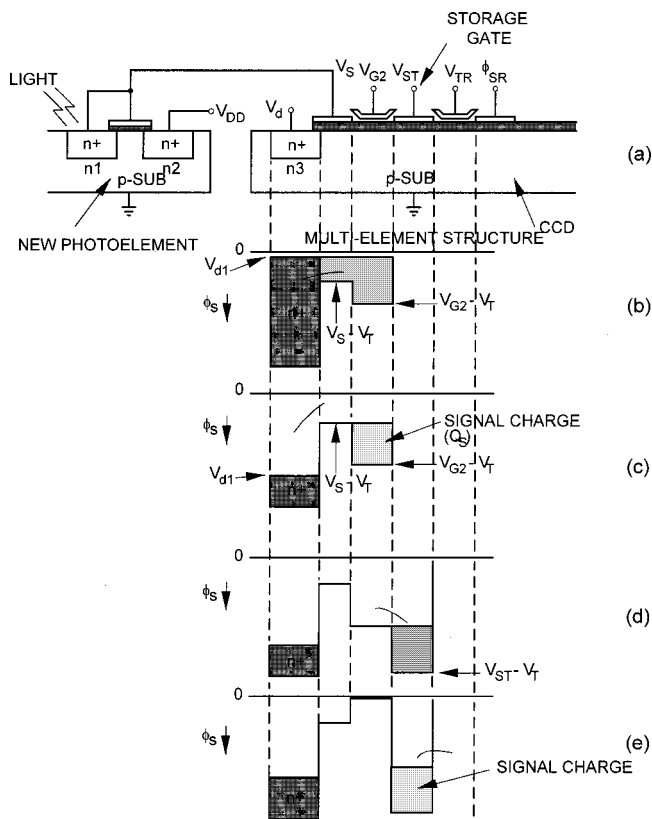


Fig. 1 PHOTOFET element.

Mead later used the parasitic vertical bipolar transistor with a logarithmic response in his silicon retinas.² The logarithmic function there is again a result of the subthreshold operation of the diode-connected MOS transistors, added in series to the bipolar transistor. The voltage output of this photoreceptor is logarithmic over four or five orders of magnitude of incoming light intensity. It was used successfully by Mahowald,³ Boahen and Andreou,⁴ and Boahen.⁵ This detector operates in the subthreshold region and has a low output voltage swing.

A disadvantage of these pixels is that this form of compression leads to low contrast and loss of details. This is the reason that adaptation, where linearity around the operation point is exploited, was proposed (as discussed next). Other disadvantages of these pixels is that the mismatch between the transistors will cause a nonlinear fixed pattern noise (FPN) and not a constant FPN at the output. Also, the response of the logarithmic pixels with this kind of readout is light dependent. This means that for low light intensities the readout time would be very slow, depending also on the photodiode capacitance.

Local adaptation was performed using a feedback mechanism to adjust the operating point of the circuit to the ambient light level in an implementation of a silicon retina.^{3,5} The computation performed is based on models of computation in distal layers of the vertebrate retina, which include the cones, the horizontal cells, and the bipolar cells. In the retina, the cones are the light detectors, the horizontal cells average the outputs of the cones spatially and temporally, and the bipolar cells detect the difference between the averaged output of the horizontal cells and the input. In the

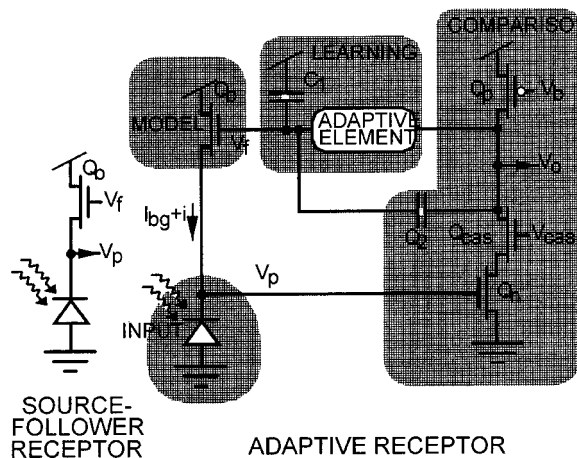


Fig. 2 Receptor circuits.

silicon retina,³ the cones are implemented using parasitic phototransistors and MOS diode logarithmic current-to-voltage converters. Averaging is performed using a hexagonal network of active resistors. The pixel output is the difference between the phototransistor value and this average, which enables contrast enhancement.

Delbruck and Mead⁶ suggested an adaptive photoreceptor with wide dynamic range with an innovative adaptive element in the feedback path (see Fig. 2). The circuit came to replace the simple nonadaptive source follower shown on the left of Fig. 2. The source follower receptor was deficient in two respects: the offsets were very large and the response was too slow. The adaptive receptor, shown on the right of Fig. 2, consists of a source follower receptor input stage combined with amplification and low-pass-filtered feedback. A conceptual way of thinking about the operation is indicated by the shaded areas. The circuit uses an internal model to make a prediction about the input signal. The output comes from a comparison of the input and the prediction. The loop is completed by using learning to refine the model so that predictions become more accurate. The level adaptation in the adaptive receptor is a simple type of learning. This photocircuit can adapt to steady state (or long-term) light intensity variations through a logarithmic transfer function. At higher frequencies the gain of the circuit is boosted. This is so since an adaptive element and a capacitor divider are used in the feedback loop from the input of the amplifier. Also, the cascode transistor was added to nullify the Miller capacitance from the gate to drain of Q_n and to double the amplifier gain. The circuit is therefore capable of providing high gain for short-term signals, while long-term signals are logarithmically compressed. The adaptive element provides an effective resistance that is huge for small signals and small for large signals. Hence, the adaptation is slow for small signals and fast for large signals. For a detailed explanation of the adaptive element see Ref. 6. The drawbacks are large area and leakage current, which could mean scene-dependent noise, since the adaptive element does not give us 0 V at zero current.

An inherent disadvantage of adaptive sensors is that the image cannot be reconstructed easily, due to the adaptation!

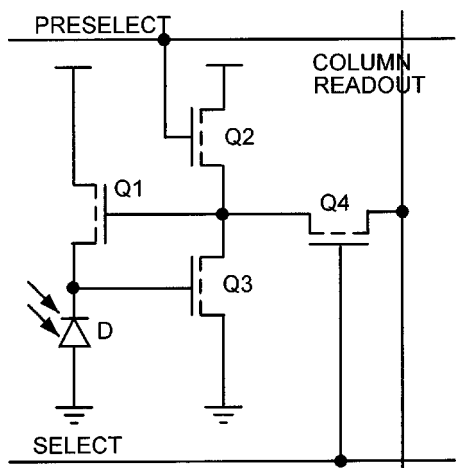


Fig. 3 Schematic of a logarithmic pixel cell.



(a)



(b)

Fig. 4 Same scene imaged by (a) a CCD sensor and (b) a CMOS logarithmic sensor (thanks to Dr. Huppertz from Fraunhofer Institute).

In this example, the frequency-dependent gain would have to be taken into account.

The Huppertz et al.⁷ circuit is very similar to Delbruck's circuit without the adaptive element (see Fig. 3). The pixel contains a photodiode and an amplifier Q_2 and Q_3 with a feedback MOS transistor Q_1 operating in weak inversion. As the feedback maintains almost a constant voltage across the photodiode, the capacitance of the photodiode is ineffective and the circuit exhibits a very high frequency bandwidth. Therefore, an advantage of the Huppertz et al. circuit is that the parasitic capacitor does not affect low-light-level performance and the operation is a lot faster. Reported frame rate is 150 f/s for a 128×128 imager at 1 W/m^2 .

As with other logarithmic sensors, this sensor works in continuous time. This means a higher sampling rate could be achieved. However, the SNR is relatively low, i.e., around 56 dB. This is so because the pixel is not integrating (averaging) the signal and improving the SNR is proportion to the root of the frame time. In this specific sensor, the mismatch in voltage is doubled. Here two transistors Q_1 and Q_3 contribute to the mismatch, not just one transistor. An example of two pictures of the same scene, one taken by a CCD and the other by a logarithmic CMOS sensor is shown in Fig. 4.

Takada and Miyatake⁸ showed a logarithmic converting CCD line sensor that has better noise performance for low light levels (40 dB at 0.1 lx). The reason for the improved SNR is that the sensor performs integration on a capacitor and hence the time constant is larger, which makes the bandwidth smaller.

A classical configuration of a logarithmic sensor was implemented⁹ by IMEC. The conversion of (photo) current to an output voltage could be achieved through a series resistor. However, since the photocurrent is low (femtoampere to nanoampere range), the value of the series resistance must be very high. The resistor was therefore realized as a metal-oxide semiconductor field effect transistor (MOSFET) resistor configuration (Fig. 5). Since this MOSFET operates in weak inversion, the photocurrent conversion to voltage is also logarithmic. The time constant equals 0.14 ms, as opposed to a few milliseconds integra-

tion time in integrating sensors. This enables 4.5M pixels/s of this $2K \times 2K$ sensor.

Lately, a big debate in the imaging community concerns linear versus nonlinear, namely logarithmic, sensors.¹⁰ The drawbacks for the logarithmic approach are that nonlinear output makes subsequent signal processing (e.g., for color) difficult, contrast ratio is sacrificed, and FPN is increased, therefore dynamic range is low, and (typically) there is large temporal noise. Also, with scaling, V_{th} becomes lower and the subthreshold characteristic might get worse, i.e.,

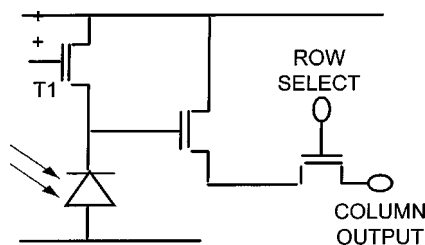


Fig. 5 Logarithmic pixel architecture.

there will be more mismatch, more FPN, and therefore a lower dynamic range. The continuous reading is claimed to be "true random access." However, with this type of sensors, adaptation is low and proportional to the light level. Thus, the appealing potential of scanning virtually anytime is not practical. In practice, for room light level, roughly 1 ms is required.

Drawbacks of the linear approach are that if the sensor is going to be used by humans, the visual system responds in a logarithmic way in any case! Also, for the display of information (on a monitor, for example), compression will be required.

This debate continues, and it seems that the application requirements are the main drive behind the sort of sensor developed. For instance, whether the application benefits from knowledge of absolute illumination levels or if contrast enhancement is the main requirement and relative illumination is sufficient etc. Decisions are made per mission, i.e., the sensor is chosen if it best fits for use in the specific task.

3 "Clipped" Sensors

The second method discussed in the literature is clipping, based on antiblooming. Blooming is an apparent increase in the size of an image of a bright object under overload conditions. In a CCD, excess carriers from a localized overload can diffuse through the bulk to neighboring potential wells and the displayed image will show artifacts in the scene as column or line defects around the highlight. This spillover of excess electrons to other pixel is called blooming.¹¹ Antiblooming techniques were proposed to suppress this spreading. Overflow drains were suggested as a means of suppression¹² in the form of reverse-biased diodes or other conductive areas between the integration sites. The overflow barrier potential can be established in several possible ways (see Fig. 6). The simplest approaches use a light-channel-stopping implant [Fig 6(a)] or a thick oxide region [Fig. 6(b)] along the overflow drains. A commonly used approach, requiring an extra level of metallization, places a special threshold electrode (horizontal gate) underneath the transfer electrodes [Fig 6(c)]. The potential barrier underneath this horizontal gate can be influenced by the gate voltage and set to be the highest of all pixels' surroundings. Thus excess electrons will spill over the lowest barrier (highest potential) and arrive at the antiblooming drain. The main drawback of the horizontal overflow drain is its occupation of the silicon area, which normally belongs to the light-sensitive pixel. A vertical, i.e., "in depth," overflow drain has also been introduced. The vertical antiblooming structure is located underneath the photodiode, and it decreases the visible long-wavelength sensitivity of the photosensor site.

Clipping is performed using an antiblooming structure.^{1,13} In conjunction with their PHOTOFET (see Fig. 1) Chamberlain and Lee¹ used an antiblooming structure. At required intervals the diode $n3$ is pulsed by V_d close to ground where it fills up with electrons the potential wells of both the V_S and V_{G2} gates. This is shown schematically in Fig. 1(b). Then V_d is taken to a positive potential (V_{d2}) where the excess electrons are scooped out [Fig. 1(c)] leaving behind the signal charge $Q_s = (V_{G2} - V_S)C_{ox}$, where C_{ox} is the gate oxide capacitance of

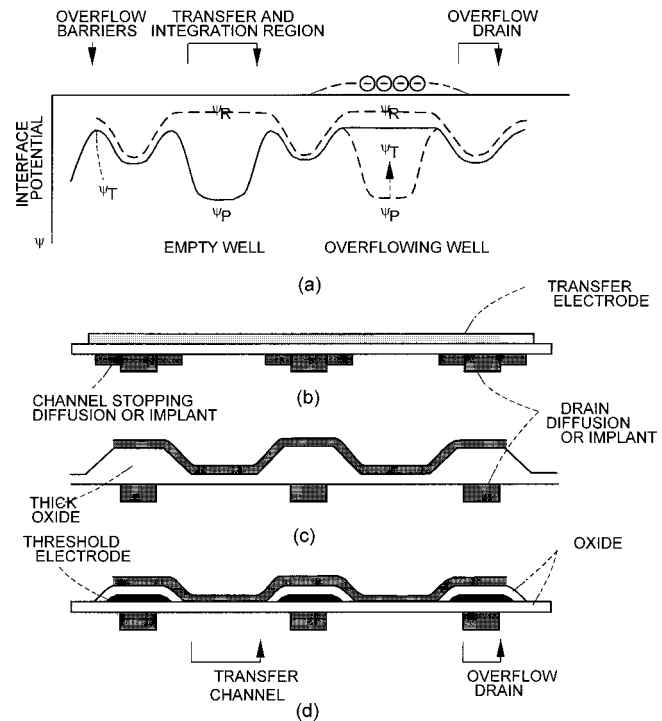


Fig. 6 Overflow drains.

V_{G2} . The next stage involves transferring this charge to the storage (V_{ST}) gate, as shown in Fig. 1(d). Then V_{G2} is lowered while the signal charge is transferred in a conventional way to the CCD readout shift register. Chan et al.¹³ used an extra gate, which is turned on to dump the extra charge such that only the well charge that can be handled is available for readout. The disadvantage of these approaches is that they require a decrease in the fill factor or a larger pixel.

Kub and Anderson¹⁴ showed an improved version of a compressing photodetector using the subthreshold conducting effect. The photodetector is similar to conventional CCD imagers except that the blooming gate is biased with a small potential offset between the blooming and imaging gates. At high photocurrent levels, the photocarriers are injected from the imaging gate region over the blooming gate potential barrier into the drain, resulting in a slowing of the rate of photocarrier accumulation with increasing photocurrent. The slowing of the rate of carrier buildup with increasing photocurrent results in a compressive transfer characteristic. The mechanism of photocarrier injection over the blooming gate potential barrier (Fig. 7) is similar to subthreshold conduction in the MOS transistor. The time at which transition from integration to compression occurs depends on when subthreshold conduction becomes dominant, which happens faster for long interrogation periods (see Ref. 14 for the details). This is the main improvement this sensor has over previous logarithmic sensors—the integration portion of the transfer characteristic is smaller relative to the compressive portion, for most cases.

Decker and Sodini¹⁵ and Decker et al.¹⁶ exploited the use of the overflow gate using a technique described by Sayag.¹⁷ The voltage applied to the overflow gate changes over the integration period, thus changing the height of the

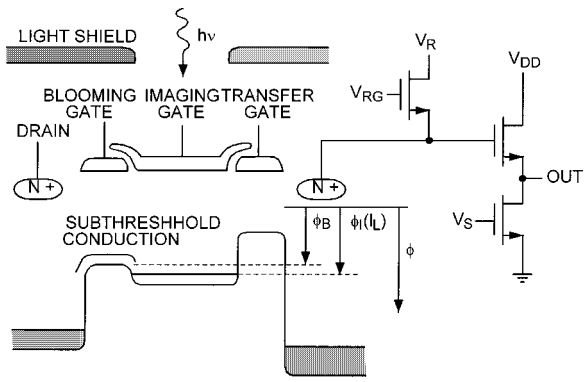


Fig. 7 Compressing photodetector using the subthreshold conducting effect: cross section (upper), schematic (right), and electric potential (lower). Arrows indicate electronic potential; electronic potential in imaging gate region, $\phi_i(L)$, and electronic potential in blooming gate region, ϕ_B ; V_R , reference voltage; V_{RG} , reference gate bias voltage; V_{DD} , output circuit bias voltage; and V_S , clock voltage.

potential barrier. At each point in time, photogenerated charge in excess of the limit imposed by the barrier immediately flows over the barrier into a charge sink. Figure 8 shows a sample compression curve $b(t)$ expressed in terms of integrated maximum stored charge. A charge integration curve $q(t)$ shows linear integration until time t_i , barrier-limited integration from then till t_d and free integration from then until T . For any I , charge $Q(I)$ can be separated into a barrier limited component Q_{bl} and a freely integrated component Q_{free} , as shown in the figure. Any arbitrary compression characteristic can be achieved via control of the barrier. However, this requires external control over the number of steps, the duration of each step, and the barrier voltage for each step during the integration time.

Vietze and Seitz also suggested a high-dynamic-range sensor.¹⁸ The idea proposed there is to subtract an individual user-programmable offset signal over a range of seven to eight orders of magnitude with a dynamic range of 60 dB at a given parameter setting. The offset current information is locally stored on the pixel site. This method could be viewed as clipping the signal as well, and it has the advantage that the value that is passed for later processing has more information, since it is not merely the full-well value passed when overflow exists. The output provided after subtraction is linear, while the programmable offset current can be programmed over a range of more than 7 decades. The downside is that initialization must be

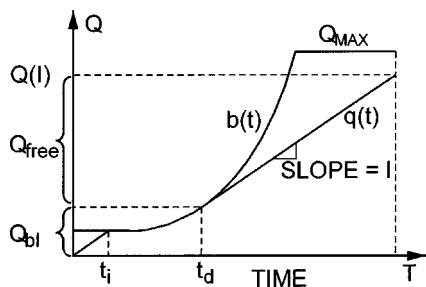


Fig. 8 An example of compression and charge integration curves.

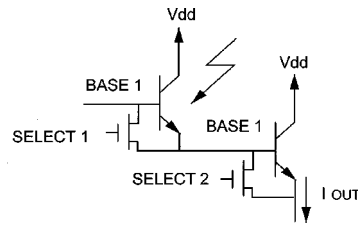


Fig. 9 Multisensitivity photodetector.

done, and space is taken for in-pixel storage. The noise reported is 600 μV at zero offset current, which results in 67 dB for the photodetector. With the programmed offset current the dynamic range was reduced to 55 to 60 dB, since there was additional noise in the gate voltage controlling the current source transistor, depending on the offset current.

4 Multimode Sensors

Ward et al.¹⁹ proposed a multisensitivity photodetector. The detector is a parasitic vertical bipolar between diffusion, well, and substrate. By connecting a MOS transistor to the base and emitter of the bipolar transistor in a Darlington structure the current gain can be boosted once more. Thus, both bipolar transistors can be activated at very low light intensities and inactivated at higher intensities. For midlevels, only one bipolar transistor is activated. Two selection transistors are required within the pixel to choose the mode and, of course, the area this pixel occupies is very large (see Fig. 9).

Deval et al.²⁰ proposed another version of this multimode sensor. Their version selects between bipolar and diode modes. The selection is done automatically (not during the frame time). Sixteen transistors are required in the pixel, which means a fairly low fill factor.

5 Frequency-Based Sensors

Yang²¹ proposes to use a pulse photosensor that uses simple integrate and reset circuitry to directly convert optical energy into a pulse frequency output that can vary over five to six orders of magnitude and is linearly proportional to optical energy (see Fig. 10). With this approach, the pixel fill factor is much decreased, since the inverter chain resides next to the photodiode. Also, the pulse timing relies on the threshold voltages of the inverters. Since threshold voltage mismatch exists between different transistors, there will be a different response for each pixel. This makes this sensor worse in terms of noise, since the

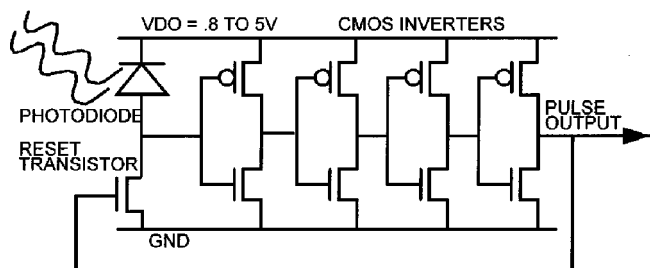


Fig. 10 Pulse photosensor with reset circuitry.

threshold mismatch translates to a multiplicative error (the output frequency of the pulses is affected) and not just constant FPN.

Boahen designed a pixel circuit that senses, amplifies, filters, and quantizes the visual signal.⁵ The transducer is a vertical bipolar transistor; its emitter current is proportional to the incident light intensity. Two current-spreading networks diffuse the photocurrent signals over time and space. The result is a spatiotemporally bandpass filtered image. A separate layer computes a measure of the local light intensity, and feeds back this information to the input layer, where the intensity information is used to control light sensitivity. The result is local automatic gain correction (AGC). A pulse generator converts current from the excitatory layer into pulse frequency. The diode capacitor integrator computes a current that is proportional to the short-term average of the pulse frequency; this current is subtracted from the pulse generator's input. The difference becomes larger as the input changes more rapidly, so pulses are fired more frequently. Hence, the more rapidly the input changes, the more rapidly the pulse generator fires. The pixel also performs adaptive quantization; the details can be found in Ref. 5. The main drawback, again, is the spatial resolution.

Seitz and Raynor²² proposed a new light frequency sensor. In this circuit, the voltage across the reverse-biased p - n junction is kept constant to ensure that the optoelectronic properties are independent of light level. The maximum SNR was 67 dB and pixel size was 27×60 m in a 2- μ m process.

6 Control of Integration Time

The other method mentioned in the literature is controlling the integration time. Global control over integration time was achieved via mechanical irises and electronic shuttering.^{23,24} The simplest implementation is the electronic shutter. By integrating all pixel values in a frame time and calculating the average intensity, the exposure time is changed globally (i.e., for all pixels). CMOS sensors with global shuttering was proposed.²⁵⁻²⁷ If there is a large intrascene dynamic range, however, this will not be sufficient since part of the sensors might get saturated and white or black patches will be seen in the picture. In astronomy applications, star tracking for instance, a target can become very bright, as in the case during a close approach to an asteroid or comet nucleus.²⁸ Then, if the brightest pixel contains a full capacity of electrons, other pixels will contain significantly less and will therefore exhibit reduced SNRs. To overcome this limitation, local control over integration time can be implemented.

6.1 Local Exposure Control

Local exposure control attempts have also been made. These solutions usually require a large reduction in fill factor, which is problematic in many applications, for example the star tracking application.²⁹

In an adaptive sensitivity CCD image sensor that was suggested,^{30,31} each pixel has the ability to be reset at a specific time according to a control word. The control word is supplied by the computer after calculation over several frames. The design requires an AND gate and an SR flip-flop in each cell, which makes the fill factor very low.

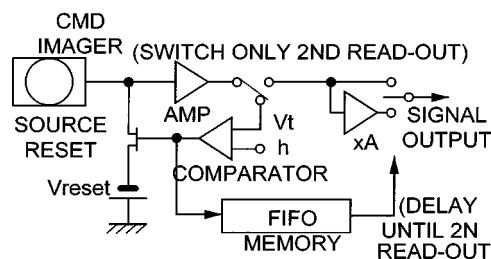


Fig. 11 CMD with dynamic range expansion.

Washkurak and Chamberlain have suggested a CCD programmable photodetector where responsivity could be controlled.³² A switched CCD network discards a fraction of the signal charge into a drain and by that increasing the dynamic range.

A dynamic range expansion method for charge-modulation device (CMD) imagers was proposed and an exponential circuit was evaluated.³³ It applies a first scan that checks if accumulation at a pixel is excessive. If so, the overexposed pixel is reset using the source reset method during the readout period. This method enables each pixel charge in the CMD device to be reset by external circuits. A first in first out (FIFO) memory holds a bit for each pixel reset/nonreset data and during a second readout an external amplifier switches its gain depending on an output from the FIFO memory (see Fig. 11).

In CMOS technology, a multiple-integration-time photoreceptor, developed at Carnegie Mellon University,³⁴ has multiple integration periods, which are chosen depending on light intensity to avoid saturation. When the charge level becomes close to saturation, the integration is stopped at one of these integration periods, and the integration time is recorded. The pixel includes two photodiodes (see Fig. 12). The photodiode a (Pd-a) detects saturation and the photodiode b (Pd-b) stores photoelectrons as a signal. Pd-a is connected to an inverter, which thresholds the Pd-a voltage. The output of the inverter is latched to control the gate connecting Pd-b to a storage capacitor (CAP1), which integrates signal charge. The latch output thus controls the integration periods. The latch output is also used for sample-holding a ramp voltage to record the integration period in the capacitor (CAP2). The area of this computational pixel is around 100×100 m and the fill factor is very low.

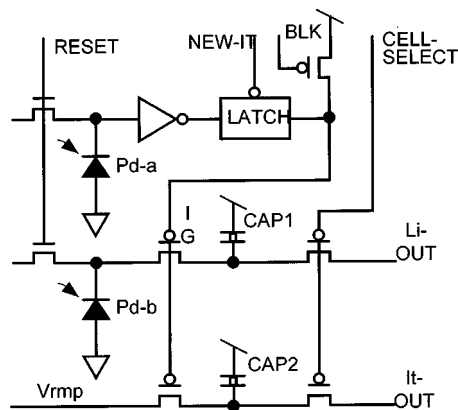


Fig. 12 Multiple-integration-time photoreceptor.

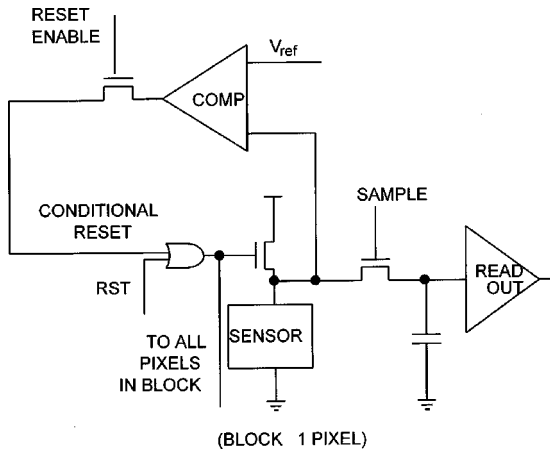


Fig. 13 Automatic wide-dynamic-range sensor control pixel.

Locally adaptive active pixels²⁰ were also proposed. One proposed circuit adapts the shutter timing. This circuit requires one frame time to “adapt,” i.e., set the adequate time out of three possible ones. The pixel control is quite expensive in area: 10 transistors are required in this pixel.

6.2 Real-Time Autonomous Control over Integration Time

The proposed automatic wide-dynamic-range sensor^{35,36} consists of a two-dimensional array of sensors, each capable of being exposed for a different length of time—autonomously controlled on-chip. Reset enable pulses are generated at specific times during the integration period. At each reset enable point, a nondestructive readout is performed on the sensor and compared to a threshold value. A conditional reset pulse is generated if the sensor value exceeds the threshold voltage (see Fig. 13).

A fairly new CCD approach that uses two storage sites per interline transfer CCD pixel has been reported where two signals from two integration intervals within the frame period are stored.³⁷ The short exposure time is fixed, however, and corresponds to the vertical clock period. This “Hyper-D range” (see Fig. 14) CCD architecture requires complicated CCD pixel design with a low fill factor and requires twice the charge transfer speed for CCD readout. The density of the pixels is doubled, and eight clock phases are used to produce two different exposure times, which are superimposed at the readout. For low lights, this sensor gives a worse response since the effective area for collection is reduced. An improved design presented³⁸ in 1997

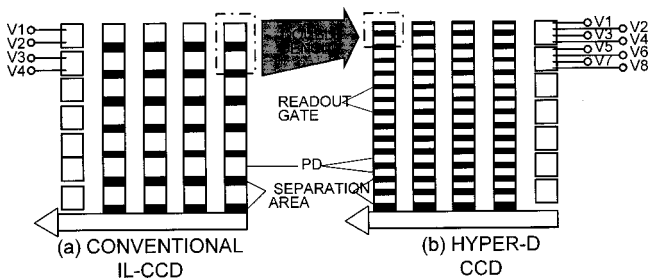


Fig. 14 Hyper-D CCD.

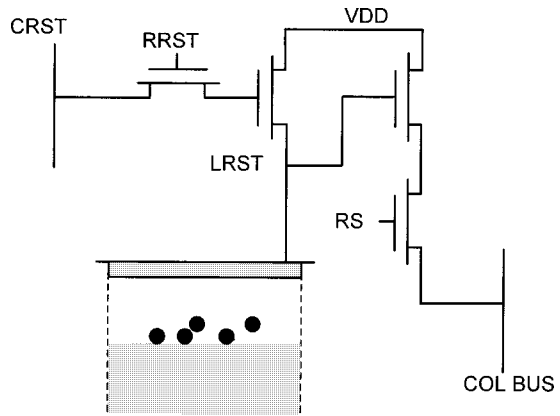


Fig. 15 Individual pixel reset circuit.

included technological modifications that made the well hold the same nominal charge as the undivided original pixel, and the power dissipation also got lowered.

Hamamoto et al.³⁹ suggested a motion-adaptive image sensor that also detects saturation and consequently resets the pixel. This group had worked on pixel parallel and column parallel approaches for achieving this goal.

The main drawback with these solutions is the extent of the additional circuitry’s effect on spatial resolution.

7 APS Chips with Wide Dynamic Range

With the advent of CMOS technology and APSs, the integration of additional functions on-chip was exploited. One of the first functions to be researched was an APS with local control over integration time. The application was space, specifically star tracking, for which more details can be found elsewhere.⁴⁰

A traditional APS pixel⁴¹ includes a photogate, a single reset transistor, and readout source-follower circuitry. A photodiode-type APS does not use a photogate, and was previously used for random access image sensors.²⁶ Since all reset transistor gates in a given row are connected in parallel, the entire row is reset when the reset line is activated. The integration period is the time from pixel reset to pixel readout. So that pixels on the same row can have different integration periods and do not saturate, individual pixel reset (IPR) is required.

A simple way to implement IPR would be to put a second transistor in series with the row reset transistor, activated by a vertical column reset signal. Unfortunately, this has been shown to introduce reset anomalies when it has been used in CMOS readout circuits for IR focal-plane arrays for astronomy.⁴² This is believed to be due to charge pumping from the output node to the reset drain.

7.1 APS IPR

In our work,⁴³ IPR was implemented via a simple configuration of two reset transistors, as illustrated in Fig. 15. The column reset (CRST) and row reset (RRST) lines must both be at a logical high voltage to activate the reset transistor. This simple configuration enables low noise, anomaly-free readout and the implementation of a smaller pixel with higher fill factor compared to previously reported efforts for local exposure control, as previously described.

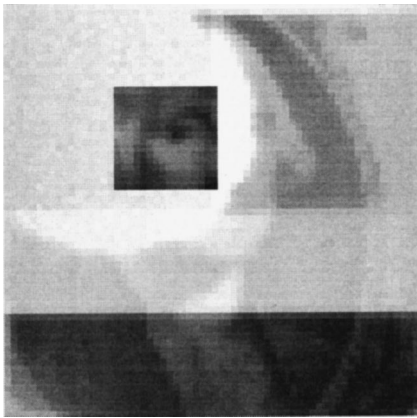


Fig. 16 Sensor output with a region of short integration time through George Washington's eye.

A prototype chip with the pixel-resetting circuitry confirmed the operability of the individual pixel reset operation. Six different variations of the pixel design were explored, and this is the reason for observing six different responsivities for the different parts of the array (see Fig. 16).

A subarray was selected for additional reset. This resulted in a less-exposed region. The output image example is shown in Fig. 16. The darker region across the image represents pixels that were reset during the nominal integration time, so that they had a shorter effective integration time. Some pixels in the rest of the image appear saturated, or white. The linearity of the “electronic shutter” operation was measured to be quite good.⁴³ The main disadvantage of this design, however, is that it requires at least one additional frame time to adjust the exposure time to each pixel appropriately. This was overcome in the solution described next.

7.2 Dual Sampling

In 1997 two groups came up with a similar idea for widening the dynamic range. The first was Olympus⁴⁴ with a CMD sensor and the second was the Jet Propulsion Laboratory⁴⁵ (JPL) with an APS sensor. I concentrate here on the JPL approach—the dual sampling approach. As emphasized here, however, the Olympus approach is very similar.

7.2.1 Dual-sampling approach

In the traditional photodiode-type CMOS APSs operating in normal mode,⁴⁶ a particular row is selected for readout. The sensor data from the selected row is copied simultaneously for all columns onto a sampling capacitor bank at the bottom of the columns. The pixels in the row are then reset and read a second time, and a new integration is started. The capacitor bank is then scanned sequentially for readout. This scan completes the readout for the selected row. The next row is then selected and the procedure repeated.

The row readout process thus consists of two steps: The “copy” step, which takes time T_{copy} , typically 1 to 10 μs , and the readout scanning step, which takes time T_{scan} , typically 100 ns to 10 μs per pixel. If there are M pixels in

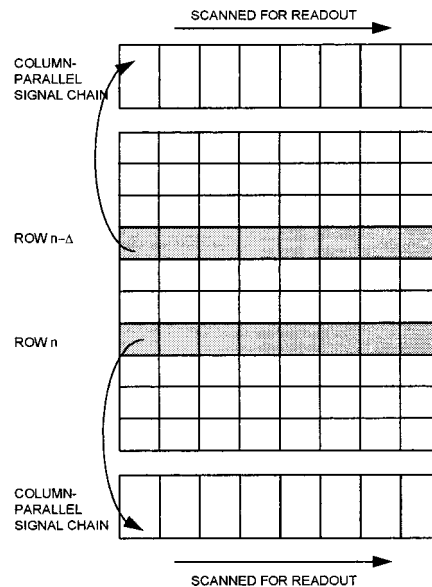


Fig. 17 Schematic illustration of dual-sample, dual-output imager architecture.

a row (i.e., M columns), then the total time for row readout, T_{rro} , is $T_{rro} = T_{copy} + MT_{scan}$. The total time to readout a frame with N rows is $T_{frame} = nT_{rro}$. This time is also the integration time for the conventional CMOS APS.

The architecture of the recently proposed⁴⁵ wide intrasene dynamic range (WIDyR) approach is shown in Fig. 17. In the new architecture, a second column signal processing chain circuit has been added to the upper part of the sensor. As before, row n is selected for readout and copied into the lower capacitor bank. Row n is reset in the process. Immediately following, however, row $n - \Delta$ is selected and copied into the upper capacitor bank. Row $n - \Delta$ is also reset as a consequence of being copied. Both capacitor banks are then scanned for readout. The row readout time has now been increased according to:

$$T'_{rro} = 2T_{copy} + MT_{scan}.$$

Since $MT_{scan} \gg T_{copy}$ in most cases, $T'_{rro} \approx T_{rro}$. The total time to read out a frame is also insignificantly affected. However, the integration time for pixels copied into the lower capacitor bank is given by

$$T1_{int} = (N - \Delta)T'_{rro},$$

and the integration time for the pixels read into the upper capacitor bank is

$$T2_{int} = \Delta T'_{rro}.$$

The output data thus contains two sets of pixel data: one taken with integration time $T1_{int}$, and the second with time $T2_{int}$. For example, when $N = 512$ and $\Delta = 2$, then the ratio of $T1_{int}:T2_{int}$ is 255:1. The intrasene dynamic range capability of the sensor is extended by the factor $T1_{int}/T2_{int}$.

The Olympus solution takes advantage of the nondestructive readout (NDRO) of the CMD. The sensor is also



Fig. 18 Experimental sensor outputs with dual sampling with four row delay yielding exposure ratio of 15:1 for two different levels of faceplate illumination. The left images are the output of short integration channel, and the right images are the output of long integration channel. The upper pair has lower faceplate illumination than the lower pair. Note vertical shift between the left and right images corresponding to a four-row delay.

scanned twice a field. The first scanning outputs a signal with a short exposure time in NDRO mode. The second scanning outputs a long exposure signal with the conventional reset operation.

7.3 Experimental Results

The sensor was operated in WIDyR mode using the dual outputs. An example of the output is shown in Fig. 18 for a short integration period (left) and a long integration period (right), where the two outputs are four rows apart, improving the intrascene dynamic range by 15:1 or 3.75 bits.

Off-chip fusion of the two images can be performed either linearly (e.g., bit concatenation) or nonlinearity (e.g., addition). Olympus synthesized the two signals to generate an image. The reproduced image has a dynamic range of 84 dB and an example is shown in Fig. 19.

The dual-sampling approach offers several important advantages over the previous approaches described earlier in the paper. First, the linearity of the signal is preserved. Second, no modification to the standard CMOS APS pixel is required to achieve a high dynamic range so that the fill factor and the pixel size can be optimized. Third, the low read noise of the CMOS APS pixel is preserved.

The drawbacks of this solution are that two integration times are used. If the illumination level does not suit one of these, information will still be lost. Outputting more than two integration times would require an additional analog memory on-chip to synchronize these outputs. This would add area, therefore causing a smaller field of view.

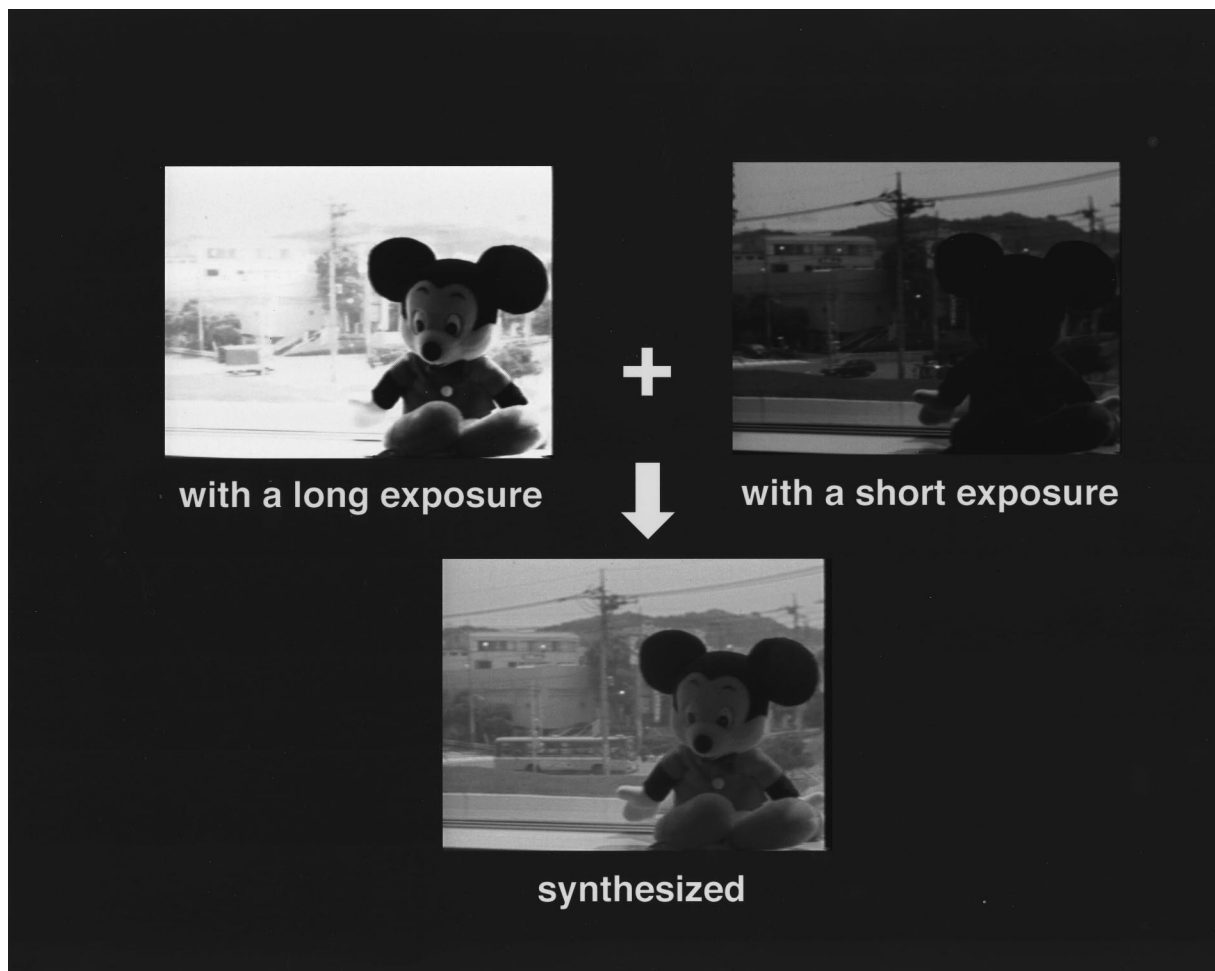


Fig. 19 Off-chip fused pictures (thanks to Olympus Company).

7.4 Exposure Control Limitations

Changing the exposure time enables us achieve a wider dynamic range (by changing the gain of the photocurrent conversion to voltage). Since the exposure time can be precisely controlled, the intensity is proportional to the output voltage divided by the exposure time. What is changed in this process though is the intensity resolution; small variations in intensity that we were able to view with the normal (long) exposure time, might be lost within the noise in a short exposure time. However, since the main noise source in imaging devices is the shot noise, the meaningful signal is only above noise, i.e., above the square root of the signal. Any resolution beyond the noise level is not effective.

What this means is that although the wide dynamic range of input requires a large number of bits (greater than 14) in an analog-to-digital converter (ADC) to cover the low and the extreme high levels, the resolution in which we acquire each of these extreme values is different. For the high illumination levels, the extreme resolution might not be effective at all, and unresolved within the noise.

A possible way to deal with this wide dynamic range with nonlinear effective resolution, is to amplify the signal by different amounts and select the most appropriate level by converting each in turn. A parts-efficient way is to enable the control of the gain of a single amplifier.

Another solution is to make the ADC nonlinear so that it responds to a strong signal with less sensitivity than to a weak signal. This brings up a compression curve. For low input values, a change of 1 bit of output corresponds to a small input change, but for large input values a much larger input difference is needed for the same effect, i.e., the least significant bit (LSB) changes in weight according to the input.

Yet another solution, currently being researched⁴⁷ at Ben-Gurion University (BGU), is to sample the sensor output multiple times during the integration time, so as to find the right ranging of a linear analog-to-digital (AD) conversion taking place. This could result in a huge increase of the dynamic range, since the representation of the value could be described as floating point: the ADC value is the mantissa, while the ranging is the exponent.

Once we have the information, the matter is displaying it "properly." Future research developments will probably tackle that.⁴⁸ In contrast to the photodetectors, which offer a single compression curve, with the wide-dynamic-range linear photodetectors any compression curve that is best suited for the specific application can be used.

8 Summary

Previous and current techniques to increase the dynamic range of image sensors were discussed, including linear and nonlinear approaches, and trade-off issues were pointed out. The nonlinear sensors, namely logarithmic ones, have a main disadvantage of low contrast. Adaptive sensors were described, where the sensor performed linearly over a small range around the operating point. In scenarios where the absolute illumination is important, the adaptation means loss of information. Integrating sensors have the ability to extend the dynamic range in a linear way via control of integration time. This control can be achieved globally or locally, automatically or manually (i.e., by the microprocessor), in the same frame time (i.e., real time) or longer.

Most of the proposed solutions required a high sacrifice in fill factor or spatial resolution. Two recent APS solutions with a wide dynamic range based on altering the exposure time were described and experimental results shown. The main advantage of these solutions is that they require only a small payment in fill factor (first solution) or no sacrifice at all in fill factor (second solution). However, further research must be done to provide a real-time solution that covers the illumination levels in an exhaustive way.

In general, the control of integration time can be viewed as a form of gain control. As such, like every system with gain control, there is a trade-off in SNR and intensity resolution. Future trends were discussed, mainly in terms of how to enable a wide dynamic range with the appropriate intensity resolution.

Acknowledgments

The author would like to thank Ali Mioni, Brita Olson, Junichi Nakamura, and Eric Fossum for valuable discussions. In addition many thanks to Mr. Tsutomu Nakamura for making Olympus pictures available and to Dr. Jurgen Huppertz for making IMS pictures available for this manuscript.

References

1. S. G. Chamberlain and J. P. Lee, "Silicon imaging arrays with new photoelements, wide dynamic range and free from blooming," in *Proc. 1984 Custom Integrated Circuits Conf.*, pp. 81–85, Rochester, NY (1984).
2. C. Mead, "A sensitive electronic photoreceptor," in *Proc. 1985 Chapel Hill Conference on VLSI*, H. Fuchs, Ed., pp. 463–471, Computer Science Press, Rockville, MD (1985).
3. C. Mead, *Analog VLSI and Neural Networks*, Addison Wesley, Reading, MA (1989).
4. K. A. Boahen and A. G. Andreou, "A contrast sensitive retina with reciprocal synapses," *Adv. Neural Inf. Process.* **4**, 762–772 (1992).
5. K. A. Boahen, "The retinotopic approach: pixel parallel adaptive amplification, filtering, and quantization," *Analog Integr. Circuits Signal Process.* **13**, 53–68 (1997).
6. T. Delbruck and C. Mead, "Adaptive photoreceptor with wide dynamic range," in *Proc. IEEE Intl. Symp. on Circuits and Systems*, pp. 339–342, London, UK (1994).
7. J. Huppertz, R. Hauschild, B. J. Hosticka, T. Kneip, S. Muller, and M. Schwarz, "Fast CMOS imaging with high dynamic range," in *Proc. 1997 IEEE Workshop on Charge-Coupled Devices and Advanced Image Sensors*, Bruges, Belgium (1997).
8. K. Takada and S. Miyatake, "Logarithmic converting CCD sensor and its noise characteristics," in *Proc. 1997 IEEE Workshop on Charge-Coupled Devices and Advanced Image Sensors*, Bruges, Belgium (1997).
9. B. Dierickx, D. Scheffer, G. Meynants, W. Ogiers, and J. Vlummens, "Random addressable active pixel image sensors," *Proc. SPIE* **2950**, 2–7 (1996).
10. E. R. Fossum, "Non-linear output from image sensors: applications, techniques, and limitations," Discussion topic at the 1997 IEEE Workshop on Charge-Coupled Devices and Advanced Image Sensors, Bruges, Belgium, June 5–7, 1997.
11. A. J. P. Theuwissen, *Solid-State Imaging with Charge-Coupled Devices*, Kluwer Academic (1995).
12. C. H. Sequin and M. F. Tompsett, *Charge Transfer Devices*, Academic Press (1975).
13. T. Chan, O. R. Barrett, C. W. Chen, Y. Abbendini, and D. D. Wen, "A 488×430 Interline Transfer CCD imager with integrated exposure and blooming control," *Proc. 1984 IEEE Intl. Solid State Circuits Conf.*, pp. 30–31, San Francisco, CA (1984).
14. F. J. Kub and G. W. Anderson, "Compressing photodetectors for long optical pulses using a lateral blooming drain structure," *IEEE Trans. Electron Devices* **40**(10), 1740–1744 (1993).
15. S. Decker and C. G. Sodini, "Comparison of CCD and CMOS pixels for a wide dynamic range area imager," presented at 1995 IEEE Workshop on CCDs and Advanced Image Sensors, April 20–22, 1995, Dana Point, CA.
16. S. Decker, R. McGrath, K. Brehmer, and C. Sodini, "A 256×256 CMOS imaging array with wide dynamic range pixels and column parallel digital output," in *Proc. ISSCC 1998*, pp. 176–177 (1998).

17. M. Sayag, "Non-linear photosite response in CCD imagers," U.S. Patent No. 5055667 (1984).
18. O. Vietze and P. Seitz, "Active pixels for image sensing with programmable, high dynamic range," *Proc. SPIE* **2654**, 93–98 (1996).
19. V. Ward, M. Syrzycki, and G. Chapman, "CMOS photodetector with built in light adaptation mechanism," *Microelectron. J.* **24**(5), 547–553 (1993).
20. A. Deval, A. Khan, and L. A. Akers, "Locally adaptive active pixel sensors," in *Proc. of ISCAS 1997*, Vol. 1, pp. 685–688 (1997).
21. W. Yang, "A wide-dynamic-range, low power photosensor array," in *Proc. IEEE ISSCC*, Vol. 37 (1994).
22. P. Seitz and J. M. Raynor, "A linear array of photodetectors with wide dynamic range and near quantum-noise limit," *Sens. Actuators A* **61**, 327–330 (1997).
23. B. L. Cochrun, "Linear infrared charged coupled device focal plane with programmable stare time," *Proc. SPIE* **501**, 157–163 (1984).
24. D. E. Caudle, "New generation gated intensified camera," *Proc. SPIE* **569**, 107–113 (1985).
25. T. Kinugasa et al., "An electronic variable-shutter system in video camera use," *IEEE Trans. Consum. Electron.* **CE-33**, 249–258 (Aug. 1987).
26. O. Yadid-Pecht, R. Ginosar, and Y. Shacham-Diamand, "A random access photodiode array for intelligent image capture," *IEEE Trans. Electron Devices* **38**(8), 1772–1781 (1991).
27. C. A. Huat and B. A. Wolley, "A 128×128 pixel standard CMOS image sensor with electronic shuttering," *Proc. ISSCC*, pp. 180–181 (1996).
28. R. H. Stanton, J. W. Alexander, E. W. Dennison, T. A. Glavich, and L. F. Hovland, "Optical tracking using charge coupled devices," *Opt. Eng.* **26**(9), 930–938 (1987).
29. E. R. Fossum, R. K. Bartman, and A. Eisenman, "Application of the active pixel sensor concept to guidance and navigation, in space guidance, control, and tracking," *Proc. SPIE* **1949**, 256–265 (1993).
30. S. Chen and R. Ginosar, "Adaptive sensitivity CCD image sensor," *Proc. SPIE* **2415**, 303–309 (1995).
31. R. Ginosar and A. Gnusin, "A wide dynamic range CMOS image sensor," in *Proc. 1997 IEEE Workshop on Charge-Coupled Devices and Advanced Image Sensors*, Bruges, Belgium (1997).
32. B. Washkurak and S. Chamberlain, "A switched CCD electrode programmable photodetector," presented at 1995 IEEE Workshop on CCD's and Advanced Image Sensors, April 20–22, 1995, Dana Point, CA.
33. H. Shimamoto, K. Mitani, and Y. Fujita, "A dynamic range expansion method for a CMD imager," *Proc. SPIE* **3019**, 249–255 (1997).
34. R. Miyagawa and T. Kanade, "Integration time based computational image sensor," presented at 1995 IEEE Workshop on CCD's and Advanced Image Sensors, April 20–22, 1995, Dana Point, CA.
35. O. Yadid-Pecht, "Widening the dynamic range of pictures," *Proc. SPIE* **1656**, 374–382 (1992).
36. O. Yadid-Pecht, "Method and apparatus for increasing the dynamic range of optical sensors," Israeli Patent No. 100620 (Feb. 1995).
37. H. Komobuchi, A. Fukumoto, T. Yamada, Y. Matsuda, and T. Kuroda, "1/4 inch NTSC format hyper-D range IL-CCD," presented at 1995 IEEE Workshop on CCDs and Advanced Image Sensors, April 20–22, 1995, Dana Point, CA.
38. T. Yamaguchi, I. Shimizu, K. Hnmi, H. Tanaka, T. Tanaka, H. Matsumaru, M. Miyashita, I. Ihara, S. Tashiro, M. Yamanaka, Y. Nishi, K. Tachikawa, and H. Komobuchi, "A 2V driving voltage 1/3 inch 410k-pixel hyper-d range CCD," in *Proc. 1997 IEEE Workshop on Charge-Coupled Devices and Advanced Image Sensors*, Bruges, Belgium (1997).
39. T. Hamamoto, K. Aizawa, and M. Hatori, "Motion adaptive image sensor," in *Proc. 1997 IEEE Workshop on Charge Coupled Devices & Advanced Image Sensors*, Bruges, Belgium (1997).
40. C. C. Clark, O. Yadid-Pecht, E. R. Fossum, P. Salomon, and E. Dennison, "Application of APS arrays to star and feature tracking systems," *Proc. SPIE* **2810**, 116–121 (1996).
41. S. E. Mendis, Kemeny, and E. R. Fossum, "CMOS active pixel image sensor," *IEEE Trans. Electron Devices* **41**(3), 452–453 (1994).
42. C. Jorquera, C. Beichman, C. Bruce, N. Gautier, and T. Jarrett, "Integration and evaluation of a near infrared camera utilizing a HgCdTe NICMOS3 array for the Mt. Palomar 200-inch observatory," in *Infrared Detectors and Instrumentation*, *Proc. SPIE* **1946**, 534–546 (1993).
43. O. Yadid-Pecht, B. Pain, C. Staller, C. Clark, and E. Fossum, "CMOS active pixel sensor star tracker with regional electronic shutter," *IEEE J. Solid-State Circuits* **32**(2), 285–288 (1997).
44. T. Nakamura and K. Saitoh, "Recent progress of CMD imaging," in *Proc. 1997 IEEE Workshop on Charge-Coupled Devices and Advanced Image Sensors*, Bruges, Belgium (1997).
45. O. Yadid-Pecht and E. Fossum, "Image sensor with ultra-high-linear-dynamic range utilizing dual output CMOS active pixel sensors," *IEEE Trans. Electron Devices* **44**(10), 1721–1724 (1997).
46. R. H. Nixon, S. E. Kemeny, C. O. Staller, and E. R. Fossum, "128 × 128 CMOS Photodiode-type active pixel sensor with on chip timing, control and signal chain electronics," in *CCDs and Solid-State Optical Sensors V*, *Proc. SPIE* **2415**, 117–123 (1995).
47. O. Yadid-Pecht, "Method for adaptive real-time expanding of the dynamic range of optical imagers, and an optical imager using the method," patent submitted.
48. B. Pain, Private Communication.



Orly Yadid-Pecht received her BSc in 1983 from the Electrical Engineering Department at the Technion-Israel Institute of Technology, where she completed her MSc in 1990 and her DSc in 1994. She was a research associate of the National Research Council (United States) from 1995 to 1997 in the area of advanced image sensing at the Jet Propulsion Laboratory (JPL), California Institute of Technology (Caltech). In 1997 she became an assistant professor in the Electrical Engineering Department at Ben Gurion University, Israel. Her interests are smart sensors, image processing, neural nets, and pattern recognition.